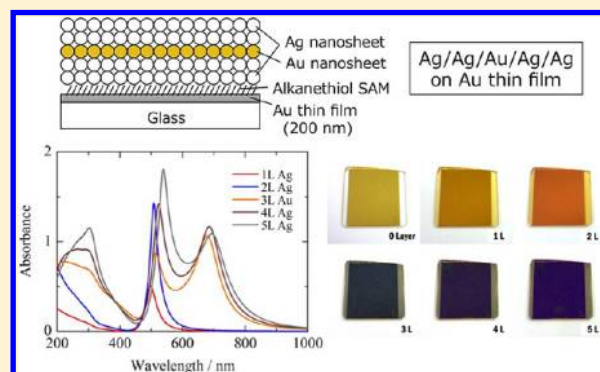


Spectroscopic Properties of Multilayered Gold Nanoparticle 2D Sheets

Akihito Yoshida, Keisuke Imazu, Xinheng Li, Koichi Okamoto, and Kaoru Tamada*

Institute for Materials Chemistry and Engineering, Kyushu University, Fukuoka 812-8581, Japan

ABSTRACT: We report the fabrication technique and optical properties of multilayered two-dimensional (2D) gold nanoparticle sheets ("Au nanosheet"). The 2D crystalline monolayer sheet composed of Au nanoparticles shows an absorption peak originating from a localized surface plasmon resonance (LSPR). It was found that the absorption spectra dramatically change when the monolayers are assembled into the multilayers on different substrates (quartz or Au). In the case of the multilayers on Au thin film ($d = 200$ nm), the LSPR peak is shifted to longer wavelength at the near-IR region by increasing the number of layers. The absorbance also depends on the layer number and shows the nonlinear behavior. On the other hand, the multilayers on quartz substrate show neither such LSPR peak shift nor nonlinear response of absorbance. The layer number dependence on metal surfaces can be interpreted as the combined effects between the *near-field* coupling of the LSPR and the *far-field* optics of the stratified metamaterial films, as proposed in our previous study. We also report the spectroscopic properties of hybrid multilayers composed of two kinds of monolayers, i.e., Au nanosheet and Ag nanosheet. The combination of the different metal nanoparticle sheets realizes more flexible plasmonic color tuning.



INTRODUCTION

In recent years, plasmonics has become one of the most active research topics in the fields of optics, physics, chemistry, etc.^{1–4} Plasmonics is based on a phenomenon so-called surface plasmon resonance (SPR), which is a specific interaction between an electromagnetic wave (light) in the visible or near-IR region and noble metals at their interface. Noble metal nanoparticles (NPs) such as Au and Ag are well-known as a good material for the excitation of localized SPR (LSPR).^{5,6} The LSPR leads to a confinement of incident light in the vicinity of the metal surface (nanoscale spaces) and excitation of enhanced electromagnetic fields as well as the large extinction of light. These interesting properties are expected to be applied to various devices such as biosensors, light emitting diodes (LEDs), solar cells, and so on.^{7–9}

To design plasmon-related optoelectronic devices, the tuning of resonance frequency is one of the most important issues. There are mainly two types of strategies to tune the frequency. One is to change the optical properties of individual NPs. The frequency of LSPR can be turned by changing the dielectric constant, size, and shape of the NPs as well as the surrounding dielectric medium.^{10–14} The second one is to utilize the two- or three-dimensionally arranged building blocks with NPs. The well-known example is a plasmon coupling, in which the frequency can be tuned by changing interparticle distance and arrangement.^{15–18}

In a previous study, our group succeeded in tuning the LSPR frequency by the use of interparticle (2D) and interlayer (3D) interaction with homogeneously sized Ag NP (Ag core size: 4.8 ± 0.1 nm).^{19,20} We found that a 2D crystalline monolayer sheet

of Ag NPs with a hexagonal structure ("Ag nanosheet") shows a large frequency shift from that of individual Ag NPs dispersed in organic solvent. We also found that the LSPR frequency of the 2D sheet can be tuned by changing the distance between adjacent Ag NPs.¹⁹ Furthermore, in our latest study, we found that the multilayered (3D structured) Ag nanosheet on metal thin film (Au and Ag) exhibits drastic changes of absorption spectra according to the number of layers.²⁰ These monolayers and multilayers composed of the metal NPs have the potential to produce a frequency-tunable wide surface with homogeneously excited plasmon-enhanced fields, which must be usable for various device applications.

In this study, we expand the study of the 2D and 3D Ag nanosheets to the system with "Au nanosheet" by expecting the tuning of resonance frequency at the near-IR region. The multilayered Au nanosheets were fabricated by the Langmuir–Schaefer method in a similar manner to the previous study. The spectroscopic properties of the multilayered Au nanosheets on quartz and Au substrate were examined by using transmission or reflection spectroscopy and they were compared with previous results of Ag nanosheets. We also report the spectroscopic properties of hybrid multilayers composed of two kinds of nanosheets, i.e., Ag nanosheet and Au nanosheet. The combination of the different metal nanoparticle sheets realizes more flexible plasmonic color tuning.

Received: September 1, 2012

Revised: November 9, 2012

Published: November 15, 2012

EXPERIMENTAL SECTION

Synthesis of Au NP and Fabrication of 2D and 3D Nanosheets. Oleyamine-capped gold NPs (AuOA NPs) were synthesized in a similar way reported by Hiramatsu et al.²¹ A 411 mg (1 mmol) sample of hydrogen tetrachloroaurate tetrahydrate (Kishida Chemical) and 5 mL of oleyamine (OA, Sigma-Aldrich) were dissolved in 45 mL of toluene (Wako). The solution was then heated to 100 °C and kept at that temperature for 1 h. The black-colored suspension obtained was further heated at 80 °C overnight. After the solution was cooled to room temperature, the obtained AuOA NP solution was washed (precipitation/redispersion) several times to remove excess oleyamine molecules. The purified AuOA NPs were redispersed in toluene. The average diameter of the obtained spherical Au NPs is 9.8 ± 1.8 nm (Figure 1A,B).

The fabrication method of AuOA NP nanosheet is similar to our reported for Ag NP nanosheet.¹⁹ A 500 μ L sample of the AuOA NP solution (~ 1 mg/mL) was spread on a water subphase in a LB trough (KSV NIMA small trough) (Figure 2A). The NPs were self-assembled at the air–water interface by hydrophobic interaction between the

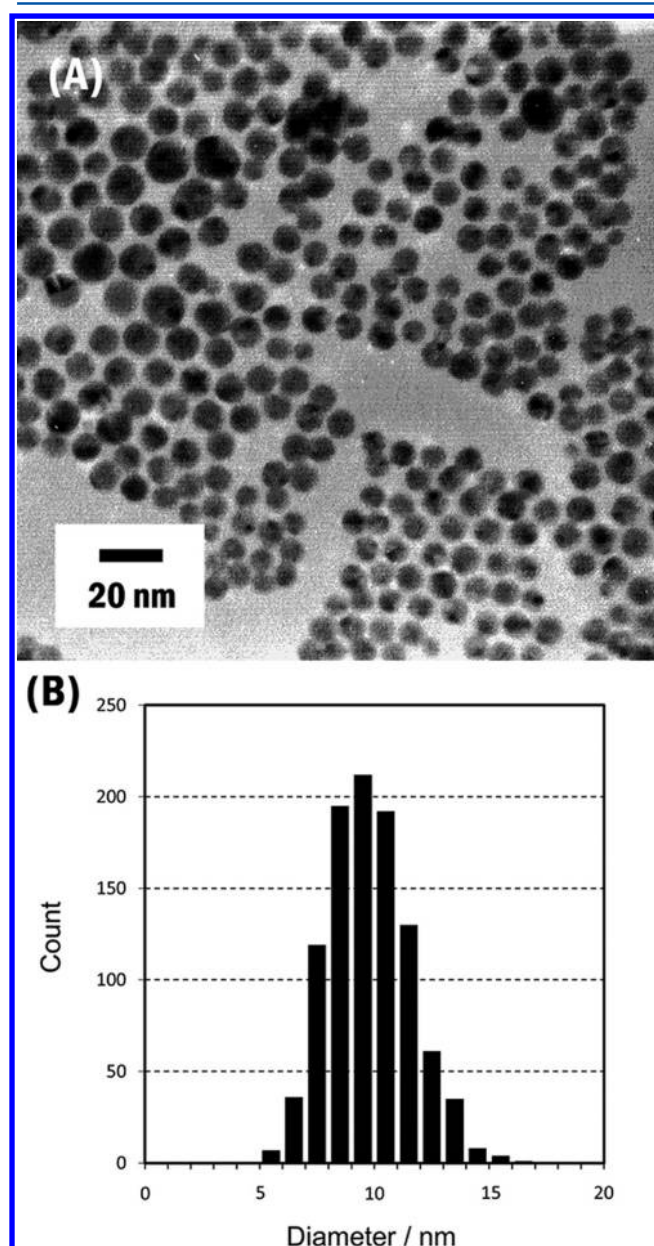


Figure 1. (A) TEM image and (B) size distribution of AuOA NPs.

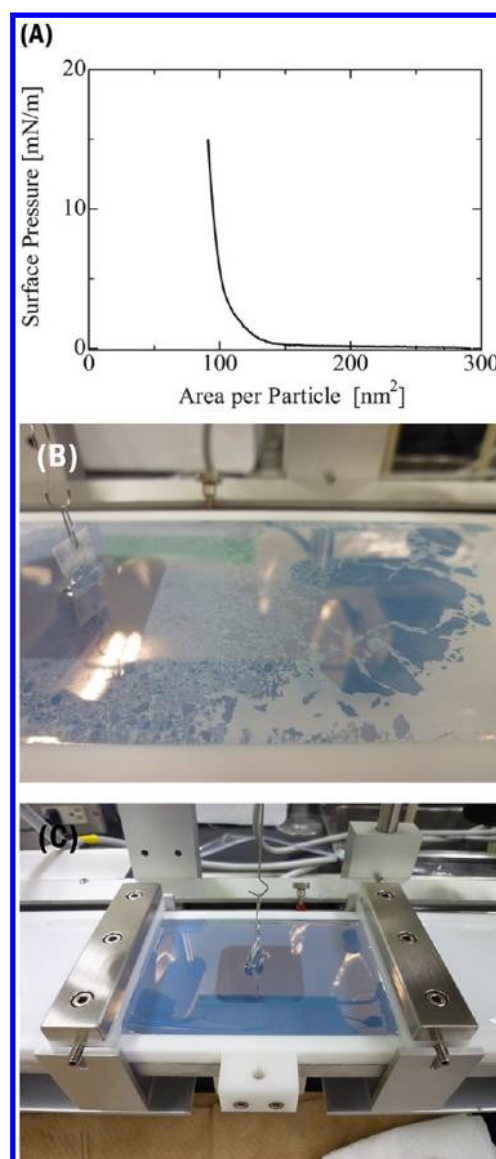


Figure 2. Formation of monolayer composed of self-assembled AuOA NPs (Au nanosheet). Π -A curve at room temperature (A) and pictures of Au nanosheet at the air–water interface before compression ($\Pi = 0$ mN/m) (B) and after compression ($\Pi = 15$ mN/m) (C).

oleylamine capping molecules and spontaneously formed solid-like domains (Figure 2B). A purple-colored homogeneous Au nanosheet (monolayer) was fabricated on the entire water surface by compression (10 mm/min) until the surface pressure (Π) reached 15 mN/m (Figure 2C). The obtained Au nanosheet was transferred to hydrophobic solid substrates (Si wafer, quartz, and Au thin film on glass) by the Langmuir–Schaefer (LS) method. The surfaces of Si wafer and quartz substrates were pretreated with hexamethyldisilazane (HMDS, Sigma-Aldrich) and the surface of the Au thin film (thickness $d = 200$ nm) was coated with 1-dodecanethiol (Sigma-Aldrich) self-assembled monolayer (SAM). The Ag nanosheet was fabricated in the same way as reported before by using 4.8 nm Ag NPs.¹⁹ Multilayered Au and Ag nanosheets were fabricated by repeating the deposition process described above.

In our previous study, it was confirmed that the ordered structure of the film is largely affected by the size distribution of the metal core and the property of organic capping molecules.¹⁹ When we performed the ligand exchange of Ag nanoparticles from myristate to alkanethiols with different chain length, the film structure became more inhomogeneous compared with that of the myristate-capped particles,

especially when short chain molecules (e.g., isobutyl mercaptan) were utilized. This is because of the smaller amphiphilic property of alkanethiols (more hydrophobic) compared with myristate, and the difficulty to form the interdigitated structures by the short chain. In the case of AuOA NPs, we could expect oleylamine to help the stable film formation by their flexible long alkyl chains. Our only concern was the bonding strength of amine on Au when AuOA NPs were spread at the air–water interface. However, the stable and reproducible Π -A isotherm of AuOA NPs proved that it was not a problem.

Characterizations. The transmission electron microscope (TEM) image of AuOA NPs was taken by a JEM-2100 (JEOL) operated at 200 kV. The sample for the TEM observation was prepared by putting a small amount of the colloidal solution on a copper grid with a collodion film (STEM100Cu, Okenshoji) and drying in air. The scanning electron microscope (SEM) image of Au nanosheet on Si substrate was taken by a SU-8000 FE-SEM (Hitachi High-Tech). All the spectra presented in this study (transmission and reflection) were acquired with a UV-1800 spectrophotometer (Shimadzu) at room temperature. A quartz cuvette with a 10 mm optical path length was used in the absorption measurement of AuOA NP solution. For the reflection measurement, the light goes into the sample surface (5 mm ϕ) with a 5° incident angle normal to the substrate with a P/N 206–14046 system. A MgF_2 -coated aluminum mirror was used as a reference.

RESULTS AND DISCUSSION

Figure 3A shows transmission absorption spectra of the AuOA NP colloidal solution and the obtained Au nanosheet

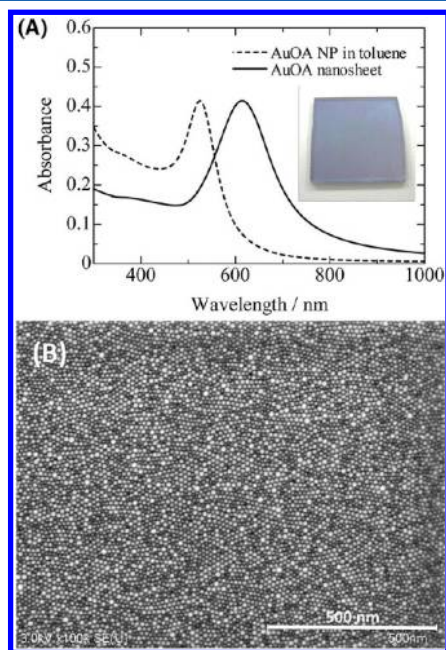


Figure 3. (A) Absorption spectra of AuOA NP colloidal solution (dashed line) and Au nanosheet on the quartz substrate (solid line). The inset is a photograph of Au nanosheet on quartz. (B) SEM image of Au nanosheet on HMDS modified Si wafer.

(monolayer) on the quartz substrate. The spectrum of AuOA NP solution (dashed line) has a peak at the wavelength of 525 nm. This peak originates from the localized surface plasmon resonance (LSPR) of the isolated Au NPs. The absorption spectrum of Au nanosheet (solid line) has a peak at a longer wavelength of 614 nm. This large red-shift ($\Delta \approx 90$ nm) should result from the formation of 2D crystalline sheet. As reported in our previous paper, the peak shift of the LSPR band in 2D crystalline sheet is expected to be much larger than that in the

1D array due to the long-range interaction of LSPR in the 2D sheet (delocalized LSPR).¹⁹ Figure 3B shows a SEM image of Au nanosheet on Si substrate. The Au NPs exhibit a close-packed structure basically although there are defects and domain boundaries on the surface more than on Ag nanosheet.²⁰ This is probably due to the size distribution of AuOA NPs and the rigidity of the particle domains. AuOA NPs is twice as large as Ag NPs so that Au nanosheet is expected to be more rigid than Ag nanosheet.

Multilayered Au nanosheets were fabricated by “stamping” the monolayer on the hydrophobic substrate in a layer-by-layer manner.²² In this study we prepared the multilayers up to 5 monolayers (5L) on quartz and Au thin film (200 nm thickness) as shown in Figure 4A. Figure 4B shows the absorption spectra of multilayered Au nanosheet on quartz substrate. The absorbance increased monotonously with the number of layers as expected, while the peak position and shape of the absorption spectra did not change so much by the multilayer formation ($\lambda_{\text{max}} \approx 610$ nm). Only a very small blue shift of the peak position was observed.

In contrast, the optical response of multilayered Au nanosheets was significant on gold thin film. The reflection spectra of the multilayered Au nanosheet on Au film are shown in Figure 5A, and the absorption spectra obtained from Figure 5A are shown in Figure 5B. Here the reflection spectrum of Au thin film was used as a reference to calculate the absorbance. For the “1 Layer sample” in Figure 5A, a dip appeared at $\lambda = 648$ nm. It was converted to the absorption peak at $\lambda = 648$ nm in Figure 5B. This peak looks similar to the monolayer on quartz substrate shown in Figure 3A. Therefore, the absorption peak around 650 nm in the reflection spectrum is ascribed to the LSPR band of the Au nanosheet. The additional red-shift ($\Delta \approx 30$ nm) on Au thin films must be attributed to the influence of metal substrate.

It is interesting that the absorption peak on Au thin film changed significantly when the second layer was deposited. The peak was shifted to longer wavelength ($\lambda = 695$ nm) unlike the case on quartz substrate (Figure 6A). In addition, the absorbance also increased drastically by the second layer deposition (Figure 6B). The absorption peaks were further shifted to longer wavelength with increasing of the layer number more than three times (about 60 nm per monolayer deposition). On the other hand, the absorbance reached a maximum at the second layer and then it gradually decreased by the additional layer depositions. These behaviors are quite different from those of the multilayered Au nanosheet on quartz substrate. Reflection photographs of the multilayered Au nanosheets on Au thin film are shown in Figure 5C. The reflected colors are between green and brown and are not significant unlike the multilayered Ag nanosheet in our previous study.¹⁹ The unclear color change is due to the shift of the LSPR absorption band to the near-IR region (>650 nm).

The results obtained here are quite analogous to that of Ag nanosheet.¹⁹ The absorption peak position and intensity of the multilayered Ag nanosheet on Au thin film are drastically changed depending on the number of layers (1–5 layers). The response of the absorption spectra was absolutely nonlinear, with maximum absorption for 2 or 3 layers. This fact suggests that the spectroscopic properties of multilayered Au nanosheet can be interpreted similarly to the properties of Ag nanosheet. With the help of theoretical simulations based on the Finite-difference time-domain method (FDTD), we previously elucidated the mechanism of the color change as follows:

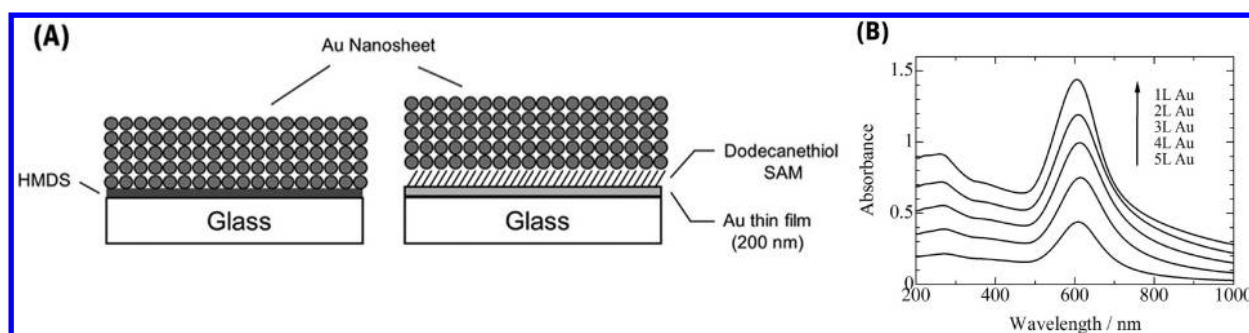


Figure 4. (A) Scheme of multilayered Au nanosheet on quartz substrates and Au thin film. (B) Absorption spectra of multilayered Au nanosheet on quartz substrate.

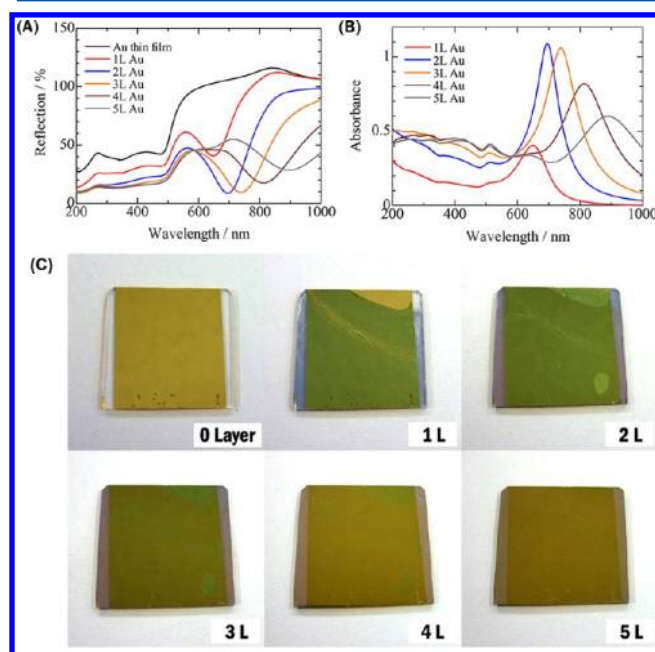


Figure 5. Reflection (A) and absorption (B) spectra of multilayered Au nanosheet on Au thin film. The absorbance values were calculated from their reflectance. (C) Reflection photographs of multilayered Au nanosheet (from 0 to 5 layers).

(1) The occurrence of the LSPR absorption peak shift results from the *near-field* electromagnetic interaction between adjacent Ag nanosheets (interlayer interaction), which is enhanced by the reflected light on the metal surface.

(2) The nonlinear behavior of absorption intensity is interpreted by the *far-field* nano-optics resulting from the metamaterial property of Ag nanosheet with the stratified structure.

Since the experimental results are similar, we consider that the explanation above for multilayered Ag nanosheet can be applied to the multilayered Au nanosheet as well. The substantial difference between Ag nanosheet and Au nanosheet is the LSPR frequency, which leads this phenomenon to the different wavelength region.

The last topic is concerned with hybrid multilayered films composed of two kinds of nanosheets, i.e., Ag nanosheet and Au nanosheet. Because both nanosheets have a hydrophobic interface, the heterogeneous deposition could be successfully done in the same way as the single-component system. The Ag/Ag/Au/Ag/Ag stratified structure on the substrate was made by 5 times deposition. Here the first 2 layers of Ag

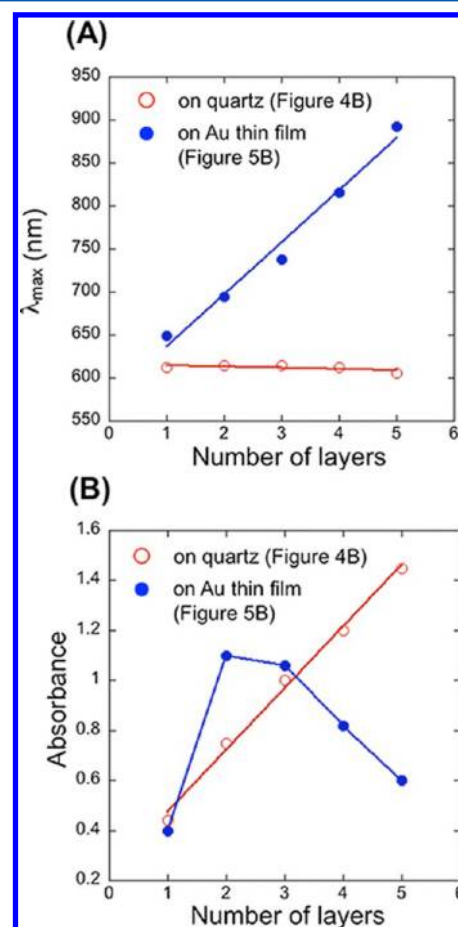


Figure 6. The LSPR peak positions (λ_{\max}) (A) and absorbances (B) of multilayered Au nanosheets against the number of Au layers on various substrates.

nanosheet were deposited, then the monolayer of Au nanosheet was deposited, and finally 2 layers of Ag nanosheet were deposited again.

The absorption spectra of these Ag/Au hybrid multilayers on quartz substrate and Au thin film are shown in Figure 7, panels A and B, respectively. The LSPR peak positions (λ_{\max}) and their absorbance originating from Ag and Au nanosheets were summarized in Figure 8A. In the same way as the multilayered Au nanosheet, the Ag/Au hybrid multilayer on quartz substrate showed only the additive spectrum of the individual layers but no additional red-shift with the increase of the layer number. On the other hand, Ag/Au hybrid multilayer exhibited a large red-shift on Au thin film, in which the additional red-shift according

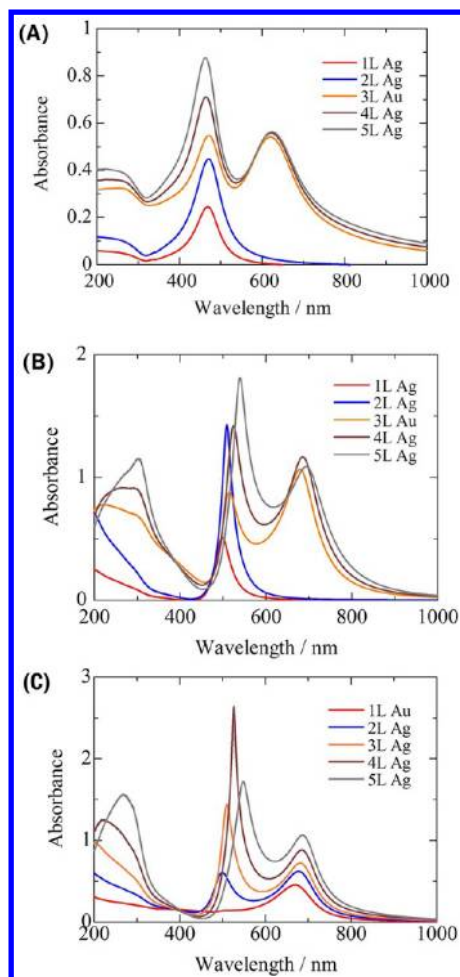


Figure 7. Absorption spectra of hybrid multilayers (Ag/Au/Ag/Au/Ag) on quartz substrate (A) and on Au thin film (B). Absorption spectra of hybrid multilayers (Au/Ag/Ag/Ag/Ag) on Au thin film (C).

to the layer number was observed as well. The nonlinear response of absorbance was also clear on AgNP-originating bands of the Ag/Au hybrid multilayer on Au thin film (Figure 8B). Interestingly, the peak intensity of the AgNP-originating band was attenuated when the AuNP layer was deposited as the third layer, and then increased again by the further deposition

of the fourth and fifth Ag layers. We changed the position to insert the Au layer from the third layer to the first layer (Figure 7C) and confirmed their position dependence. The absorption spectra shown in Figure 7C were quite different from that shown in Figure 7B, especially for the peak intensities. When the Au layer was deposited as the first layer, the peak intensities of AuNP-originating bands kept increasing by the deposition of AgNP layers on top. This did not happen on the AuNP-originating band inserted as the third layer. These optical responses seem to be quite complex; however, actually they can be reasonably reproduced by the FDTD calculation as reported in our previous study. When the LSPR of the particle layers are twice excited by the incident and reflected lights and the additional trapping of the light occurs in the multilayers, it is a natural result that the layer composition (the position of AuNP layer in the Ag layers) induces the spectrum change.

Reflection photographs of the Ag/Au hybrid multilayers (Ag/Ag/Au/Ag/Ag) on Au thin film are shown in Figure 9.

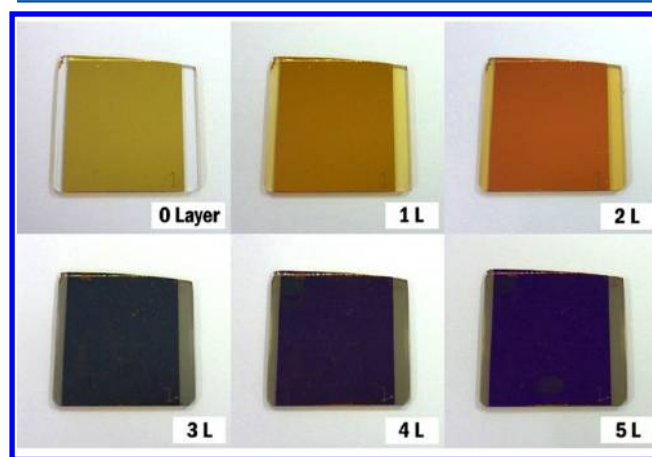


Figure 9. Reflection photographs of hybrid multilayers (Ag/Ag/Au/Ag/Ag) on Au thin film.

Compared with the single-component Au nanosheet and the previous reports for single-component Ag nanosheet,¹⁹ the Ag/Au hybrid films show the significantly wider range of colors. This color variation arises from the insertion of Au nanosheet having an absorption in relatively longer wavelength than the Ag nanosheet. This result indicates the multilayered system

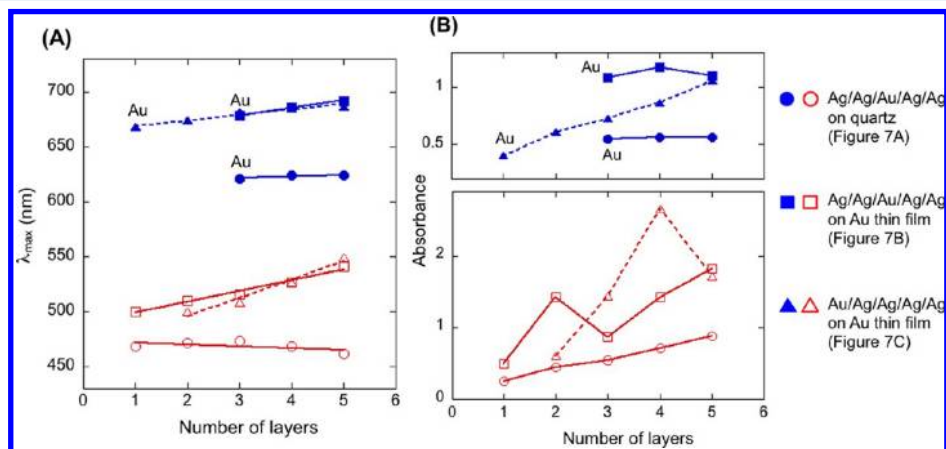


Figure 8. The LSPR peak positions (λ_{\max}) (A) and absorbances (B) of multilayered Ag/Au nanosheets against the number of Ag/Au layers on various substrates.

with appropriate combination of the nanosheet can realize the tuning of a variety of colors originating from LSPR, which must be quite useful for future applications.

At the end of discussions, we would like to add one note concerning the proper size of the particles to obtain the efficient collective excitation of LSPR within the layer and between the multilayers. When the particle size becomes larger (e.g., more than 50 nm), the scattering of light will be dominant, and the electromagnetic interaction beyond the adjacent particles and the layers hardly happens. In other words, reasonably small sized particles will be required to realize the multilayered plasmonic coating of devices.

CONCLUSION

In this study, we presented one concept to tune the LSPR frequency at the near-IR region by using a multilayered (3D) structure of Au nanoparticle sheet. It was found that the LSPR peak position of multilayered Au nanosheet on Au thin film depends on the number of layers (60 nm red-shift per layer in the near-IR region). This frequency shift results from the *near-field* electromagnetic interaction between the adjacent nanosheets (interlayer interaction) enhanced by the reflected light on the metal surface. We also showed the hybrid multilayers composed of Au and Ag nanosheet having a different LSPR frequency. We could obtain more wider and beautiful color variation in the visible region by the appropriate combination of different monolayers. The hybrid multilayers composed of 2D metal nanosheets with highly ordered structure by self-assembly have great potential for tailor-made plasmonic device applications.

AUTHOR INFORMATION

Corresponding Author

*tamada@ms.ifoc.kyushu-u.ac.jp.

Notes

The authors declare no competing financial interest.

ACKNOWLEDGMENTS

We thank Takeshi Tanaka for the technical support in TEM observation. This work was supported by the funding program for next generation world-leading researchers (NEXT program) in JSPS. K.O. acknowledges support from JST PRESTO.

REFERENCES

- (1) Maier, S. A. *Plasmonics: Fundamentals and Applications*; Springer: New York, NY, 2007.
- (2) Shvets, G.; Tsukerman, I. *Plasmonics and Plasmonic Metamaterials: Analysis and Applications*; World Scientific: Singapore, 2011.
- (3) Ozbay, E. Plasmonics: Merging Photonics and Electronics at Nanoscale Dimensions. *Science* **2006**, *311*, 189–193.
- (4) Maier, S. A.; Atwater, H. A. Plasmonics: Localization and guiding of electromagnetic energy in metal/dielectric structures. *J. Appl. Phys.* **2005**, *98*, 011101.
- (5) Kelly, K. L.; Coronado, E.; Zhao, L. L.; Schatz, G. C. The Optical Properties of Metal Nanoparticles: The Influence of Size, Shape, and Dielectric Environment. *J. Phys. Chem. B* **2003**, *107*, 668–677.
- (6) Link, S.; El-Sayed, M. A. Spectral Properties and Relaxation Dynamics of Surface Plasmon Electronic Oscillations in Gold and Silver Nanodots and Nanorods. *J. Phys. Chem. B* **1999**, *103*, 8410–8426.
- (7) Anker, J. N.; Hall, W. P.; Lyandres, O.; Shah, N. C.; Zhao, J.; Van Duyne, R. P. Biosensing with plasmonic nanosensors. *Nat. Mater.* **2008**, *7*, 442–453.
- (8) Okamoto, K.; Niki, I.; Shvarts, A.; Narukawa, Y.; Mukai, T.; Scherer, A. Surface-plasmon-enhanced light emitters based on InGaAs quantum wells. *Nat. Mater.* **2004**, *3*, 601–605.
- (9) Morfa, A. J.; Rowlen, K. L.; Reilly, T. H., III; Romero, M. J.; Lagemaat, J. V. D. Plasmon-enhanced solar energy conversion in organic bulk heterojunction photovoltaics. *Appl. Phys. Lett.* **2008**, *92*, 013504.
- (10) Lee, K. S.; El-Sayed, M. A. Gold and Silver Nanoparticles in Sensing and Imaging: Sensitivity of Plasmon Response to Size, Shape, and Metal Composition. *J. Phys. Chem. B* **2006**, *110*, 19220–19225.
- (11) Mallin, M. P.; Murphy, C. J. Solution-Phase Synthesis of Sub-10 nm Au–Ag Alloy Nanoparticles. *Nano Lett.* **2002**, *2*, 1235–1237.
- (12) Ziegler, C.; Eychmüller, A. Seeded Growth Synthesis of Uniform Gold Nanoparticles with Diameters of 15–300 nm. *J. Phys. Chem. C* **2011**, *115*, 4502–4506.
- (13) Chen, H. J.; Kou, X. S.; Yang, Z.; Ni, W. H.; Wang, J. F. Shape- and Size-Dependent Refractive Index Sensitivity of Gold Nanoparticles. *Langmuir* **2008**, *24*, 5233–5237.
- (14) Ghosh, S. K.; Nath, S.; Kundu, S.; Esumi, K.; Pal, T. Solvent and Ligand Effects on the Localized Surface Plasmon Resonance (LSPR) of Gold Colloids. *J. Phys. Chem. B* **2004**, *108*, 13963–13971.
- (15) Taleb, A.; Petit, C.; Pileni, M. P. Optical Properties of Self-Assembled 2D and 3D Superlattices of Silver Nanoparticles. *J. Phys. Chem. B* **1998**, *102*, 2214–2220.
- (16) Haynes, C. L.; McFarland, A. D.; Zhao, L. L.; Van Duyne, R. P.; Schatz, G. C.; Gunnarsson, L.; Prikulis, J.; Kasemo, B.; Käll, M. Nanoparticle Optics: The Importance of Radiative Dipole Coupling in Two-Dimensional Nanoparticle Arrays. *J. Phys. Chem. B* **2003**, *107*, 7337–7342.
- (17) Ishifuji, M.; Mitsuishi, M.; Miyashita, T. Bottom-up Design of Hybrid Polymer Nanoassemblies Elucidates Plasmon-Enhanced Second Harmonic Generation from Nonlinear Optical Dyes. *J. Am. Chem. Soc.* **2009**, *131*, 4418–4424.
- (18) Jain, P. K.; Huang, W.; El-Sayed, M. A. On the Universal Scaling Behavior of the Distance Decay of Plasmon Coupling in Metal Nanoparticle Pairs: A Plasmon Ruler Equation. *Nano Lett.* **2007**, *7*, 2080–2088.
- (19) Toma, M.; Toma, K.; Michioka, K.; Ikezoe, Y.; Obara, D.; Okamoto, K.; Tamada, K. Collective plasmon modes excited on a silver nanoparticle 2D crystalline sheet. *Phys. Chem. Chem. Phys.* **2011**, *13*, 7459–7466.
- (20) Okamoto, K.; Lin, B.; Imazu, K.; Yoshida, A.; Toma, K.; Toma, M.; Tamada, K. Tuning Colors of Silver Nanoparticle Sheets by Multilayered Crystalline Structures on Metal Substrates. *Plasmonics* **2012**, DOI: 10.1007/s11468-012-9437-2.
- (21) Hiramatsu, H.; Osterloh, F. E. A Simple Large-Scale Synthesis of Nearly Monodisperse Gold and Silver Nanoparticles with Adjustable Sizes and with Exchangeable Surfactants. *Chem. Mater.* **2004**, *16*, 2509–2511.
- (22) Kuwajima, S.; Okada, Y.; Yoshida, Y.; Abe, K.; Tanigaki, N.; Yamaguchi, T.; Nagasawa, H.; Sakurai, K.; Yase, K. Structural characterization of monolayer and regularly stacked multi-layers composed of silver nanoparticles by using X-ray reflectivity. *Colloids Surfaces, A* **2002**, *197*, 1–5.